Direct-Coupled TE–TM Dual-Mode Waveguide Cavities

Cristiano Tomassoni, *Senior Member, IEEE*, Simone Bastioli, *Senior Member, IEEE*, Richard Snyder, *Life Fellow, IEEE*, and Valentin de la Rubia

***Abstract*— This letter introduces a novel quadruplet structure in waveguide technology, comprising a dual-mode TM cavity within two λ/4 TE cavities. This structure demonstrates the capability of generating responses with four poles and two transmission zeros (TZs). Notably compact, it accommodates both wideband and narrowband responses effectively. The TZs are obtained by exploiting the nonresonating modes within the TM section. The coupling between the resonant mode of the TE section and both resonating and nonresonating modes is achieved by precise positioning of the TE section relative to the TM section. This inherent flexibility in TZ positioning renders the structure highly adaptable. Moreover, this structure can be exploited as building block for the design of higher order filters. Experimental results validate the viability and effectiveness of the proposed structure.**

***Index Terms*— Cavity resonators, direct-coupled filters, elliptic filters, nonresonating modes, waveguides.**

I. Introduction

WAVEGUIDE technology represents the best solution when low-loss filters are needed [1]. However, this often results in bulky structures. Consequently, significant efforts have been made to reduce their size. The use of TM cavities to shorten filter length was introduced in [2], along with nonresonating modes for achieving transmission zeros (TZs) in in-line configurations. Nonresonating modes have also been utilized in various geometries [3], encompassing TE cavities [4], dual-mode TM cavities [5], [6], or stubbed cavities [7]. However, these solutions typically lack wideband responses. To address this limitation and create more compact filters, structures incorporating resonant irises have been proposed in [8], [9], [10], and [11]. Nonetheless, such structures face several limitations. These stem from challenges in controlling both the resonance frequency and coupling of the irises, resulting in irises with small heights that impact the filter's Q-factor.

Manuscript received 28 February 2024; accepted 5 March 2024. Date of publication 25 March 2024; date of current version 7 June 2024. *(Corresponding author: Cristiano Tomassoni.)*

Cristiano Tomassoni is with the Department of Engineering, University of Perugia, 06100 Perugia, Italy (e-mail: cristiano.tomassoni@unipg.it).

Simone Bastioli and Richard Snyder are with RS Microwave Company, Butler, NJ 07405 USA (e-mail: sbastioli@rsmicro.com; r.snyder@ieee.org).

Valentin de la Rubia is with the Departamento de Matemática Aplicada a las TIC, ETSI de Telecomunicación, Universidad Politécnica de Madrid, 28040 Madrid, Spain (e-mail: valentin.delarubia@upm.es).

This article was presented at the IEEE MTT-S International Microwave Symposium (IMS 2024), Washington, DC, USA, June 16–21, 2024.

Color versions of one or more figures in this letter are available at https://doi.org/10.1109/LMWT.2024.3377721.

Digital Object Identifier 10.1109/LMWT.2024.3377721

Recently, an intriguing new structure was introduced [12], forming a triplet of TE–TM–TE cavities capable of three poles and a TZ. The use of waveguide TE resonating sections instead of the regular irises (allowed by a more sophisticated coupling mechanism including offset and rotations) overcomes the Q-factor limitations. This concept was further developed in [13], where the foundational triplet was utilized to create higher order filters.

In this letter, we present a novel quadruplet, which comprises a dual-mode TM cavity within two λ/4 TE cavities. The primary distinction from [13] lies in the utilization of a TM dual-mode cavity, enabling the addition of a pole and a TZ while maintaining the structure's original length. For instance, a 12-pole order filter centered at 9.5 GHz, realized using the basic triplet structure introduced in [12] and [13], would produce a response with four TZs and an estimated length of 114 mm. With the proposed quadruplet, the number of TZs would increase to 6, and the anticipated length would reduce to 86 mm, representing a reduction in length of more than 25%.

II. Basic Configuration: TE–TM Dual-Mode TE

This quadruplet configuration consists of a cascade of an input λ/4 TE cavity, a dual-mode TM cavity, and an output λ/4 TE cavity. According to the routing scheme of Fig. 1, the $TE_{101/2}$ mode (where the third index equal to 1/2 means that the cavity length is λ/4) of the TE cavities couples to both TM_{210} and TM_{120} resonant modes of the dual-mode TM cavity.

Couplings M_{S1} and M_{4L} are controlled by a classical inductive iris, whereas, according to Fig. 2, the couplings M_{12} and M_{13} (M_{24} and M_{34}) are controlled by the relative position between the TE and TM cavities. It is important to note that the inductive iris generates a low-impedance load, while the direct connection between TE and TM represents a high-impedance load for the TE cavity, this resulting in a λ/4 section resonating on the $TE_{101/2}$ resonant mode.

The coupling mechanisms between TE and TM resonators can be better understood by considering the H-field distribution of TM_{120} e TM_{210}, as illustrated in Fig. 2. For instance, when the TE cavity is centered to the TM cavity, its major size is in the horizontal position ($p = 0$ and $\varphi = 0$). The $TE_{101/2}$ mode of the TE cavity couples solely with the TM_{120} ($M_{12} \neq 0$) due to the alignment of their respective transverse H-fields. Conversely, it remains completely uncoupled to the TM_{210} ($M_{13} = 0$), which possesses an orthogonal H-field.

By shifting the TE cavity toward the upper part of the TM cavity ($\varphi = 0$, $\theta = 90°$, and increasing p), the coupling to

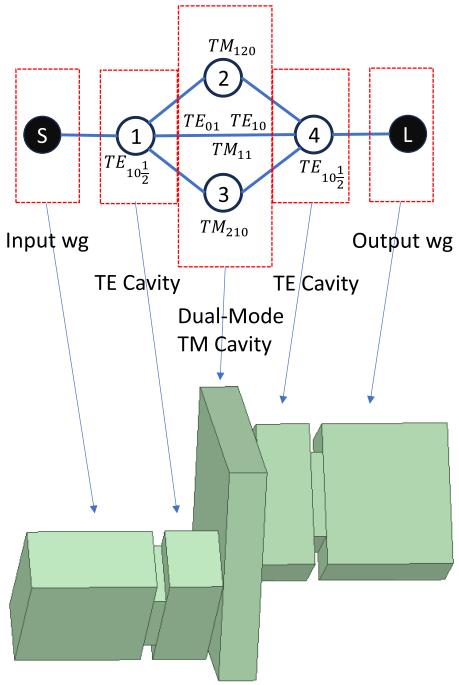

Fig. 1. Three-dimensional view of the basic TE–TM dual-mode TE structure and relevant routing scheme.

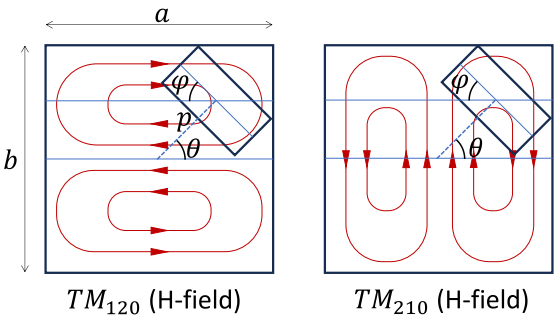

Fig. 2. Sketch depicting the coupling mechanism between the TE cavity mode and TM cavity modes M_{12} and M_{13} (M_{24} and M_{34}).

the TM_{120} decreases and reaches zero when $p = b/4$. In this position, the TM_{120} H-field is zero. As the offset p continues to increase, the coupling begins to increase again. A similar effect occurs when varying p at $\varphi = 90°$ and $\theta = 0$. In this scenario, TM_{210} is coupled ($M_{13} \neq 0$), while TM_{120} remains uncoupled ($M_{12} = 0$). A particularly intriguing scenario for our structure occurs when $\varphi = 45°$ and $\theta = 45°$ and a = b (this last assumption is very close to what happens in the practical case). Here, due to symmetry, the coupling to the two TM modes is identical ($M_{12} = M_{13}$). Also, in this configuration, the coupling values for both modes can be adjusted by varying the offset p. Moving away from this configuration, decreasing θ ($\theta < 45°$) or increasing φ ($\varphi > 45°$) will lead to an increase in M_{13} and a decrease in M_{12}. Conversely, increasing θ ($\theta > 45°$) or decreasing φ ($\varphi < 45°$) will result in a decrease in M_{13} and an increase in M_{12}. Essentially, this mechanism enables independent adjustment of M_{12} and M_{13}.

Comprehending the cross-coupling M_{14} between the modes in the two TE cavities requires visualizing both the two TE sections and the three propagating modes in the TM cavity responsible for the cross-coupling. This is shown in Fig. 3. It is important to note the mirrored configuration of the output

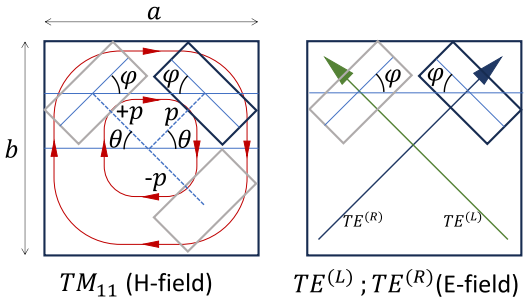

Fig. 3. Sketch depicting the coupling mechanism between the TE cavity resonant modes (M14) through the TM cavity nonresonant modes.

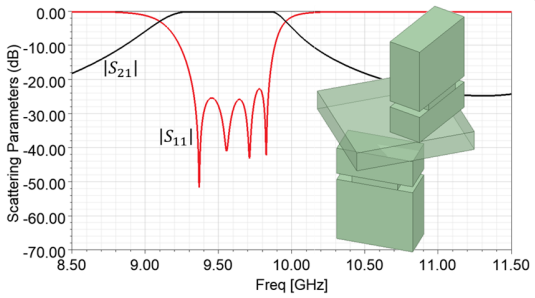

Fig. 4. Response of the proposed quadruplet with no TZs.

TE cavity concerning the input TE cavity. This configuration allows for the establishment of the following equalities: $M_{12} = M_{24}$ and $M_{13} = -M_{34}$, which are necessary to achieve a single-band response within our routing scheme. The cross-coupling mechanism functions as follows: the $TE_{101/2}$ mode in the input TE section stimulates the propagating modes in the TM cavity [TM_{11}, $TE^{(L)}$, and $TE^{(R)}$]. The propagating modes reach the output TE section and excite its $TE_{101/2}$ resonant mode. The contribution of the TM_{11} propagating mode to the cross-coupling M_{14} amplifies with an increase in the offset p, corresponding to the rise in the H-field strength of the TM_{11} mode. It is noteworthy that altering the offset from positive (+p) to negative (−p) for the output TE section can reverse the direction of this contribution, because of the inversion of the H-field direction with respect to the waveguide section.

An additional contribution to the M_{14} cross-coupling comes from the TE propagating modes [$TE^{(L)}$ and $TE^{(R)}$] in the TM cavity polarized along the diagonals (these can be regarded as a linear combination of the TE_{10} and TE_{01} modes). When $\varphi = 45°$, the input $TE_{101/2}$ mode exclusively couples with the $TE^{(R)}$, which cannot stimulate the output $TE_{101/2}$ mode that is solely linked to the $TE^{(L)}$ mode. As a result, this configuration yields no contribution to M_{14}. Conversely, when $\varphi \neq 45°$, both the input and output TE sections couple with both $TE^{(L)}$ and $TE^{(R)}$ modes. This leads to a positive contribution (when $\varphi < 45°$) or a negative contribution (when $\varphi > 45°$) to M_{14}.

Utilizing the described coupling mechanisms, several filters have been designed. Fig. 4 illustrates a response without any TZs, which depends on the sign of the M_{14} cross-coupling. As delineated earlier, the sign of M_{14} can be modified by altering the sign of the offset p in the output TE section. This approach has been employed to achieve all the responses with TZs featured in this letter.

To showcase the flexibility in the positioning of TZs, Fig. 5 displays a scenario where the TZ in the lower stopband

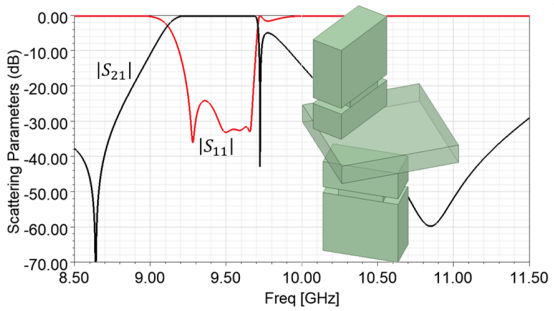

Fig. 5. Response of the proposed quadruplet with two TZs asymmetrically placed. The one in the upper stopband is closer to the filter band.

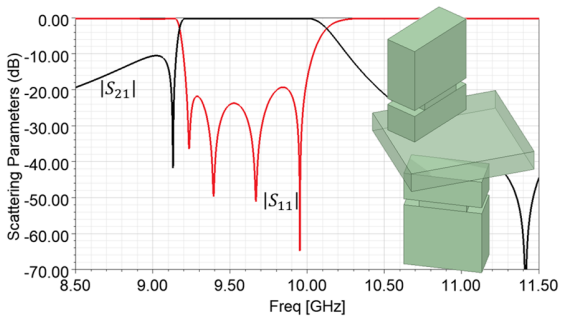

Fig. 6. Response of the proposed quadruplet with two TZs asymmetrically placed. The one in the upper stopband is closer to the filter band.

is positioned farther from the filter band, while the one in the upper stopband is in close proximity. Conversely, Fig. 6 presents the inverse pattern, with the TZ in the lower stopband positioned very close to the filter band. Finally, the manufactured filter presented in Section III shows a response where TZs are symmetrically placed concerning the filter band. The manipulation of TZ positioning has been achieved primarily by adjusting the ratio M_{12}/M_{13} (and M_{24}/M_{34}). This was primarily accomplished by altering the angle θ, based on the coupling mechanisms described previously, and optimizing the structure to attain the desired level of return loss.

III. Measurement

A four-pole filter, centered at 9 GHz with a fractional bandwidth of 6%, was designed and manufactured using the proposed quadruplet structure. The filter was fabricated employing the classical milling techniques, resulting in a highly compact design with a length of 2.83 cm. Filter dimensions are reported in Fig. 7.

Tuning screws were inserted into all the resonant cavities to achieve resonant frequency tuning. In the TM cavity, two screws were inserted into the minor and major sides, respectively, enabling independent control of the resonant frequencies of the two TM modes. No tuning screws were employed for coupling adjustments.

Fig. 8 illustrates a comparison between the simulated response (depicted by black continuous lines) and the measured responses at room temperature (indicated by red dashed lines). The excellent agreement between these responses is evident. The first spurious frequency appears at 12.2 GHz and the rejection level of the upper stopband remains below 20 dB up to 11.8 GHz.

This filter utilizes both TE and TM cavities, which exhibit different Q-factors. However, the simulated average filter

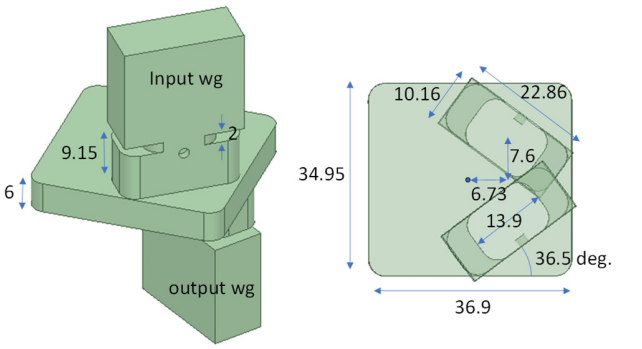

Fig. 7. Dimensions of the manufactured filters. The filter is symmetrical with respect to the central TM cavity. All reported dimensions are in millimeters, and angles are in degrees.

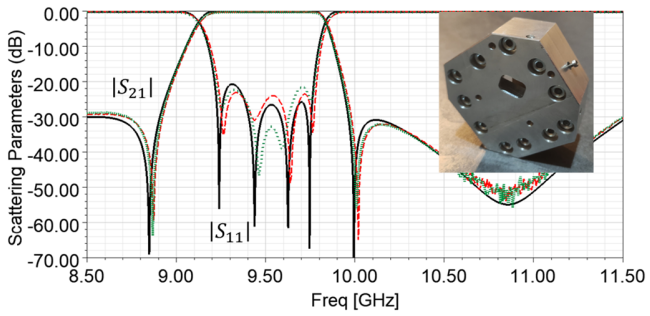

Fig. 8. Measured response of the manufactured quadruplet: comparison among room temperature measurements (red dashed lines), 90 °C measurements (green dotted lines), and full-wave simulations (continuous black lines). The photograph of the assembled filter is shown in the figure inset.

Q-factor, achieved by using aluminum with a resistivity of $5.3 \times 10^7\ \Omega \cdot m$, is approximately 4500, and the simulated insertion loss is about 0.08 dB. The measured insertion loss is approximately 0.2 dB, leading to a measured average filter Q-factor of around 2000. It must be noted that the filter was manufactured to demonstrate the feasibility of the proposed approach and was not fabricated with the aim of maximizing the Q-factor. For waveguide filters, silver plating is a standard procedure, but it was not applied in this case. Furthermore, the assembly, which plays a significant role in the measured losses, has not been optimized. Higher Q-factors can be achieved with silver plating and a better assembly design.

Furthermore, an additional measurement was conducted at 90 °C to evaluate the filter's stability under varying temperatures. The corresponding data (represented by green dotted lines) demonstrate the filter's remarkable stability. Notably, both the return loss, maintaining well below 20 dB, and the frequency shift, which remains below 10 MHz, exhibit consistent and stable performance.

IV. Conclusion

A quadruplet structure comprising a dual-mode TM cavity within two $\lambda/4$ TE cavities has been introduced. This letter covers the discussion of coupling mechanisms, showcasing several designs that highlight the structure's remarkable flexibility regarding TZ positioning and its wideband capability compared to the regular TM filters.

The manufactured prototype has been measured. It exhibits excellent agreement with the simulations. Notably, measurements taken at 90 °C showcased its temperature stability.

REFERENCES

[1] R. V. Snyder, G. Macchiarella, S. Bastioli, and C. Tomassoni, "Emerging trends in techniques and technology as applied to filter design," *IEEE J. Microw.*, vol. 1, no. 1, pp. 317–344, Jan. 2021.

[2] U. Rosenberg, S. Amari, and J. Bornemann, "Inline TM110-mode filters with high design flexibility by utilizing bypass couplings of nonresonating TE10/01 modes," *IEEE Trans. Microw. Theory Techn.*, vol. 51, no. 6, pp. 1735–1742, Jun. 2003.

[3] S. Bastioli and R. V. Snyder, "Nonresonating modes do it better! Exploiting additional modes in conjunction with operating modes to design better quality filters," *IEEE Microw. Mag.*, vol. 22, no. 1, pp. 20–45, Jan. 2021.

[4] M. Guglielmi, P. Jarry, E. Kerherve, O. Roquebrun, and D. Schmitt, "A new family of all-inductive dual-mode filters," *IEEE Trans. Microw. Theory Techn.*, vol. 49, no. 10, pp. 1764–1769, Oct. 2001.

[5] S. Bastioli, C. Tomassoni, and R. Sorrentino, "A new class of waveguide dual-mode filters using TM and nonresonating modes," *IEEE Trans. Microw. Theory Techn.*, vol. 58, no. 12, pp. 3909–3917, Dec. 2010.

[6] C. Tomassoni, S. Bastioli, and R. Sorrentino, "Generalized TM dual-mode cavity filters," *IEEE Trans. Microw. Theory Techn.*, vol. 59, no. 12, pp. 3338–3346, Dec. 2011.

[7] S. Bastioli and R. V. Snyder, "Stubbed waveguide cavity filters," *IEEE Trans. Microw. Theory Techn.*, vol. 67, no. 12, pp. 5049–5060, Dec. 2019.

[8] U. Rosenberg, S. Amari, J. Bornemann, and R. Vahldieck, "Compact pseudo-highpass filters formed by cavity and iris resonators," in *Proc. 34th Eur. Microw. Conf.*, 2004, pp. 985–988.

[9] C. Bartlett, J. Bornemann, and M. Höft, "Improved TM dual-mode filters with reduced fabrication complexity," *IEEE J. Microw.*, vol. 3, no. 1, pp. 60–69, Jan. 2023.

[10] C. Bartlett, O. Glubokov, F. Kamrath, and M. Höft, "Highly selective broadband mm-wave diplexer design," *IEEE Microw. Wireless Technol. Lett.*, vol. 33, no. 2, pp. 149–152, Feb. 2023.

[11] J. F. V. Sullca, S. Cogollos, V. E. Boria, and M. Guglielmi, "Compact dual-band and wideband filters with resonant apertures in rectangular waveguide," *IEEE Trans. Microw. Theory Techn.*, vol. 70, no. 6, pp. 3125–3140, Jun. 2022.

[12] S. Bastioli, R. Snyder, C. Tomassoni, and V. de la Rubia, "Direct-coupled TE-TM waveguide cavities," *IEEE Microw. Wireless Technol. Lett.*, vol. 33, no. 6, pp. 819–822, Jun. 2023, doi: 10.1109/LMWT.2023.3263905.

[13] S. Bastioli, R. V. Snyder, C. Tomassoni, and V. de la Rubia, "Direct-coupled TE–TM waveguide filters," *IEEE Trans. Microw. Theory Techn.*, vol. 72, no. 1, pp. 696–709, Jan. 2024.

Open Access funding provided by 'Università degli Studi di Perugia' within the CRUI CARE Agreement